Implementation of Discrete Space Vector Modulation Based Direct Torque Control of Induction Motor for Reduced Ripple: A Sliding Mode Control Approach

D. Veera 3 (M.Tech) and Dr. T. Brahmananda Reddy (Professor & Head)
E.E.E Department, G. Pulla Reddy Engineering College
Kurnool, Andhra Pradesh.

Abstract— The basic direct torque control has more torque, flux and current ripples in steady state, which results in acoustical noise and incorrect speed estimations. The main objective of this paper is to present a Discrete Space Vector Modulation based Direct Torque Controlled induction motor drive to reduce the steady state ripples. In DSVM technique, new voltage vectors are synthesized by applying three standard voltage space vectors for three equal time intervals at each sampling period. The proposed DSVM method improves the performance of the drive in terms of ripple at all modulation indices. To improve the speed performance of the drive against uncertainties caused by load disturbances, an integral switching surface sliding mode speed controller is proposed. To validate the proposed method, simulation results are presented.

Keywords: *DTC, stator flux ripple, DSVM, sliding mode control.*

I. INTRODUCTION

*I*n high-performance variable-speed drive applications for induction machines, there are two most popular control strategies: field-oriented control (FOC) and direct torque control (DTC) [1,2]. Both of them can decouple the interaction between flux and torque control, and provide good torque response in steady state and transient operation conditions. Unlike field-oriented control, direct torque control does not require coordinate transformation and any current regulator. It controls flux and torque directly based on their instantaneous errors [3]. In spite of simplicity, direct torque control is capable of generating fast torque response. In addition, direct torque control minimizes the use of machine parameters [4], so it is very little sensible to the parameters variation. Hence this control algorithm is being widely used in the industry [5]. However, the presence of torque and flux hysteresis controllers leads to variable switching frequency and also CDTC has considerable torque, flux and current ripple during steady state, which results in harmonics, power loss and incorrect speed estimation. One of the disadvantages of conventional DTC is high torque ripple [6]. Several techniques have been developed to reduce the torque ripple. One of them is duty ratio control method. In duty ratio control, a selected output voltage vector is applied for a portion of one sampling period, and a zero voltage vector is applied for the rest of the period. The pulse duration of output voltage vector can be determined by a fuzzy logic controller [7]. In Ref. [8], torque-ripple minimum condition during one sampling period is obtained from instantaneous torque variation equations. The pulse duration of output voltage vector is determined by the torque-ripple minimum condition. These

improvements can greatly reduce the torque ripple, but they increase the complexity of DTC algorithm.

An alternative method to improve the performance of CDTC in terms of torque, flux and current ripples, discrete space vector modulation (DSVM) is proposed in [9]. These results can be achieved without increasing the complexity of the power circuit and the inverter switching frequency. The new control algorithm is based on a discrete space vector modulation (DSVM) technique which uses prefixed time intervals within a cycle period. In this way a higher number of voltage space vectors can be synthesized with respect to those used in basic DTC technique. The increased number of voltage

vectors allows the definition of more accurate switching tables in which the selection of the voltage vectors is made according to the rotor speed, the flux error and the torque error. The switching tables are derived from the analysis of the equations linking the applied voltage vector to the corresponding torque and flux variations. These equations are obtained using a discrete model of the machine valid for high sampling frequency. Moreover, to reduce the torque and flux ripples, a fuzzy logic based switching table is proposed for DTC in [10]. However the presence of hysteresis controllers leads to a variable switching frequency operation. Industrial applications exhibit significant uncertainties, so that performance may deteriorate, if conventional controller such as PI controller is used. For this reasons it is worth to develop controllers that have capabilities of handling uncertainties caused by parameter variations. The sliding mode control can offer good performance against insensitivities to load disturbance [11],[12]. Hence, to improve the speed performance under uncertainties, a sliding mode speed controller is used for DTC in [13].

The main objective of this paper is to develop a discrete space vector modulation algorithm for direct torque controlled induction motor drive to reduce the steady state ripples at all modulation indices. Also to improve the speed performance, under uncertainties, an integral switching surface sliding mode speed controller is developed, which is robust under uncertainties caused by load variations.

DTC principle is described in Section II. In Section III, torque ripples in DSVM-DTC are analyzed and the optimized switching tables are defined together with integral sliding mode speed controller. Simulation results are presented in Section IV to demonstrate the performance improvements over CDTC that are obtained with proposed method. Finally conclusions are given in Section V.

II . PRINCIPLE OF CONVENTIONAL DTC

The basic block diagram representing the CDTC scheme is shown in Fig.1. The basic principle of CDTC can be explained as follows: In steady state conditions the stator and rotor flux linkage space vectors have the same angular speed and the angle δ_{sr} between these vectors determines the electromagnetic torque developed from a three-phase induction motor, according to the following expression

$$T_e = \frac{3}{2}\frac{P}{2}\frac{L_m}{\sigma L_s L_r}|\psi_r||\psi_s|\sin\delta_{sr}$$

$$(1)$$

For a given induction motor, the parameters are constant and hence T_e is the function of stator flux (ψ_s), rotor flux (ψ_r) and δ_{sr}. As the rotor time constant is large for a normal squirrel cage induction- motor, the rotor flux linkage can be assumed to be invariant in magnitude as well as in position for a small time interval. The stator flux is affected directly by impressed stator voltage

$\overline{V_s}$. Assuming the stator resistance voltage drop is small; the stator flux variation can be expressed as

$$\overline{V}_s = \frac{d\overline{\psi}_s}{dt} \text{ (or) } \Delta\overline{\psi}_s = \overline{V}_s \Delta t \qquad\qquad (2)$$
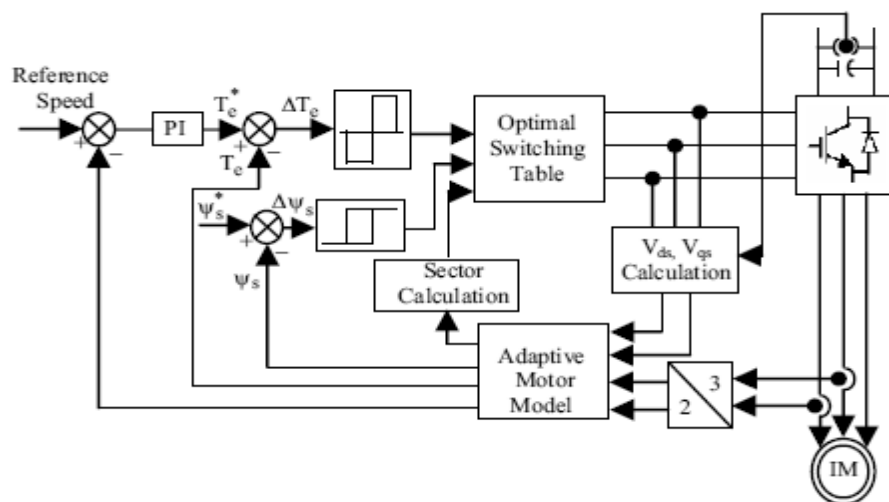

Fig.1 Block diagram of conventional DTC

Which means that $\overline{\psi}_s$ can be changed incrementally by applying stator voltage vector $\overline{V}_s$ with a time increment Δt. In order to make torque control easier, magnitude of stator flux is to be kept constant in DTC. Thus rapid changes of the electromagnetic torque can be produced by rotating the stator flux in the required direction, as directed by the torque command. The adaptive motor model takes motor currents and voltages to generate the flux, torque, speed and stator flux angle signals. The static motor data is also utilized in making calculations [5]. The estimated torque and flux are compared with their reference values in their corresponding hysteresis comparators. Finally, the outputs of hysteresis controllers with the number of sector at which the stator flux linkage space vector is located are fed to a switching table to select a suitable voltage vector to limit torque and flux errors with in the hysteresis band, which results in a direct and decoupled control.
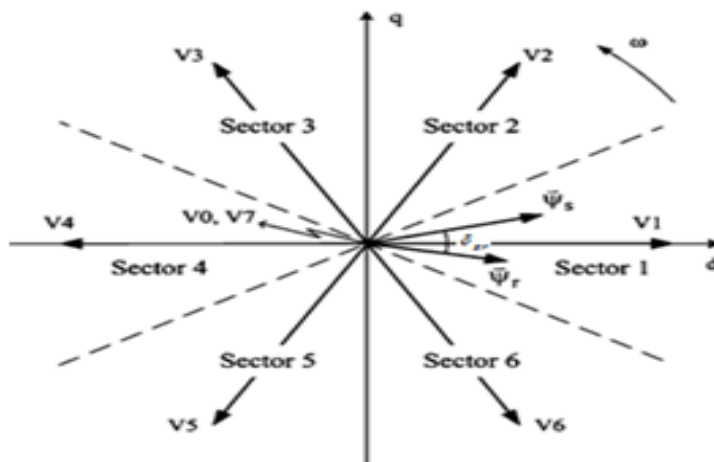

Fig.2   Eight VSI voltage vectors and six sectors.

The output of a three-phase voltage source inverter (VSI) has 8 possible voltage vectors, including 6 non-zero volt-age vectors (V1–V6) and 2 zero voltage vectors (V0, V7). The lines connecting the ends of the 6 non-zero voltage vectors constitute a hexagon. According to the positions of the non-zero voltage vectors, the d–q plane is divided into six sectors. The voltage vectors and the sectors are shown in Fig.2

III. DISCRETE SPACE VECTOR MODULATION

The major imperfection of the CDTC scheme is its limited number of voltage space vectors. Hence, the switching vectors chosen for the large errors are the same as the switching vectors chosen for small errors. To overcome this problem, it is desirable to have both the large amplitude voltage space vectors for large errors and the small voltage space vectors for small errors. For doing so, a higher number of voltage vectors with different amplitudes and positions are needed.

The DSVM algorithm uses a standard VSI and synthesizes a higher number of voltage vectors than those used in CDTC technique. In DSVM based DTC, one sampling period is divided into 'm' equal time intervals and one inverter voltage vector is applied in each of them i.e. apply 'm' voltage vectors in prefixed and equal time intervals at each sample period. The number of voltage vectors produced by the DSVM is directly proportional to the number of subdivisions 'm'. The higher the 'm', the higher the number of resultant voltage vectors; subsequently, the higher the number of voltage vectors and the lower the amplitude of current and torque ripple. However, a high number of voltage vectors require the definition of new and more complex switching tables. A good compromise between the errors compensation and the complexity of the switching tables is achieved by choosing $m=3$. Using the DSVM technique, with three equal time intervals, 36 synthesized non-zero voltage vectors can be obtained. If the stator flux vector is assumed to be in sector 1, then 19 voltage vectors can be used, as represented in Fig. 3. The black dots represent the ends of the synthesized voltage vectors. As an example, the label "23Z" denotes the voltage vector which is synthesized by using the voltage space vectors V_2, V_3 and V_Z, each one applied for one third of the sampling period.
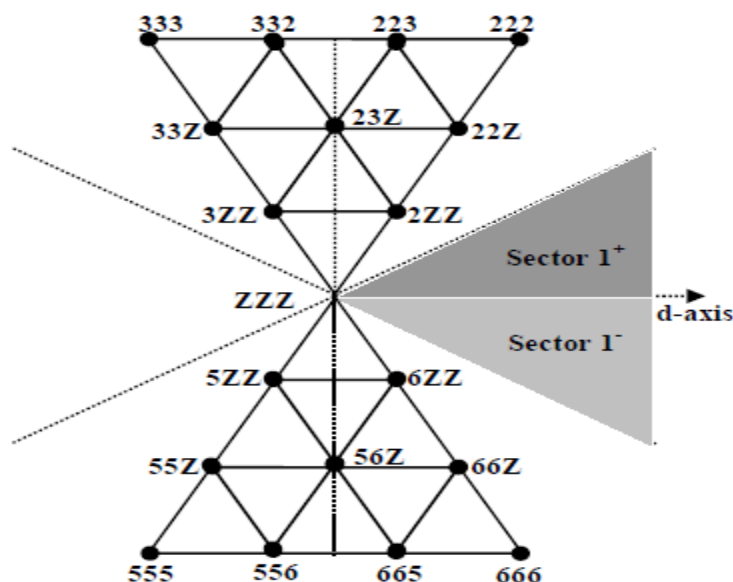

Fig.3. Synthesized voltage vectors obtained by using DSVM algorithm

In each sampling period the voltage vector is selected only once as in CDTC technique. The advantage of using the DSVM technique is that one can choose among 19 voltage vectors instead of the five of CDTC in sector 1. As a consequence, assuming the same sampling period in the two control schemes, the use of the DSVM technique improves the drive performance in terms of torque, flux and current ripple, with an increase of the inverter switching frequency. The use of the DSVM technique is very useful in applications where the maximum sampling frequency is limited by large computational time.

A. Definition of New Switching Tables:

As the torque reduction produced by the zero voltage vector is much more evident at high speed, different voltage vectors are chosen for different speed range. When the rotor speed is greater than one half of the synchronous speed, it belongs to the high-speed range. When the rotor speed is in between half of the synchronous speed and one sixth of the synchronous speed, it belongs to the medium speed range and when the rotor speed is lower than one sixth of the synchronous speed, it belongs to the low speed range. The synthesized voltage vectors are selected by a two-level flux hysteresis controller and a five-level torque hysteresis controller. The flux hysteresis controller operates according to Fig. 4.(a) and the torque hysteresis controller according to Fig. 4.(b).

The output of the flux hysteresis controller, S_ψ, has two levels. $S_\psi = 0$ means that the stator flux should be reduced and $S_\psi = 1$ means that the amplitude of the stator flux should be increased. The output of the torque hysteresis controller, S_T, has five levels. When $S_T = 1 \, or -1$, the torque needs limited or small variation and these levels will be involved in steady state operating conditions. When $S_T = 2 \, or -2$, the torque is far away from its command value and needs a large, rapid change and these levels will be involved during high dynamic transients. When $S_T = 0$, the torque is equal or close to its command value and should keep its value unchanged.
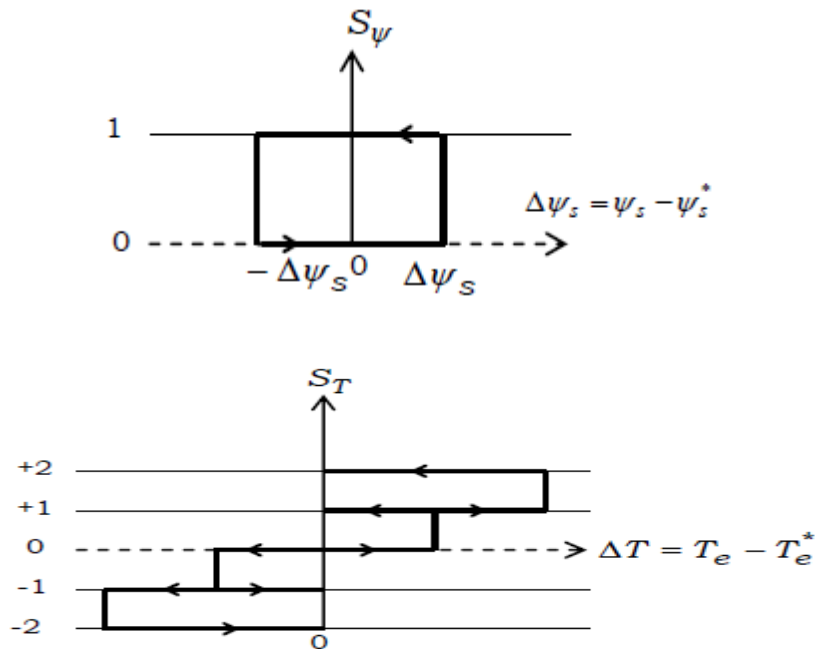

Fig.4. (a) Flux hysteresis comparator (b) Torque hysteresis comparator

Thus, based upon the outputs of the flux and torque hysteresis controllers and speed range, a suitable synthesized voltage vector will be selected from the lookup table given in Table I.

Table I. lookup table for DSVM based DTC scheme (stator flux in sector 1)

Speed range	S_ψ	S_T				
		-2	-1	0	+1	+2
Low speed range	0	555	5ZZ	ZZZ	3ZZ	333
	1	666	6ZZ	ZZZ	2ZZ	222
Middle speed range	0	555	ZZZ	3ZZ	33Z	333
	1	666	ZZZ	2ZZ	22Z	222
High speed range, sector 1+	0	555	3ZZ	33Z	333	333
	1	666	2ZZ	23Z	223	222
High speed range, sector 1-	0	555	3ZZ	23Z	332	333
	1	666	2ZZ	22Z	222	222

B. Integral Sliding Mode Speed Controller:

To improve the speed performance, an integral switching surface sliding mode speed controller is proposed, whichis robust under uncertainties caused by load torque disturbances. In general, the electromechanical equation of an induction motor is described as

$$J \frac{d\omega_m}{dt} + B\omega_m + T_L = T_e$$

(3)

Where B and J denote the viscous friction coefficient and inertia constant of the motor respectively, TL is the external load torque and ω_m is the rotor mechanical speed in angular frequency. Te is the electromagnetic torque of induction motor, defined as

$$T_e = \frac{3}{2}\frac{P}{2}\left[i_{qs}\psi_{ds} - i_{ds}\psi_{qs}\right]$$

(4)

The electromechanical equation can be modified as

$$\dot{\omega}_m + a\omega_m + d = bT_e$$

(5)

Where a=$\frac{B}{J}$, b=$\frac{1}{J}$ and d=$\frac{T_L}{J}$

Now consider the above electromechanical equation with uncertainties as

$$\dot{\omega}_m = -(a+\Delta a)\omega_m - (d+\Delta d) + (b+\Delta b)T_e$$

(6)

Δa, Δb and Δd represents the uncertainties of the terms a, b and d introduced by system parameters J and B.

Now let us define the tracking speed error further as

$$e(t) = \omega_m(t) - \omega*_m(t)$$

(7)

Where ω_m* is the rotor reference speed command.

Taking derivative of (13) with respect to time yields

$$\dot{e}(t) = \dot{\omega}_m(t) - \dot{\omega}_m^*(t) = -ae(t) + f(t) + x(t)$$

(8)

Where the following terms have been collected in the signal $f(t)$,

$$f(t) = bT_e(t) - a\omega_m^* - d(t) - \dot{\omega}_m^*(t)$$

(9)

and the $x(t)$, lumped uncertainty, defined as

$$x(t) = -\Delta a\omega_m(t) - \Delta d(t) + \Delta bT_e(t)$$

(10)

Now, the sliding variable with integral component, is defined as

$$S(t) = e(t) - \int_0^t (h-a)e(\tau)d\tau$$

(11)

where h is a constant gain. Also in order to obtain the speed trajectory tracking, the following assumptions are made.

Assumtion-1: The h must be chosen so that the term $(h-a)$ is strictly negative and hence $h<0$. Then the sliding surface is defined as follows:

$$S(t) = e(t) - \int_0^t (h-a)e(\tau)d\tau = 0$$

(12)

based on the developed switching surface, a switching control that guarantees the existence of sliding mode, a speed controller is defined as

$$f(t) = he(t) - \beta\,\mathrm{sgn}(S(t))$$

(13)

Where β is the switching gain, $S(t)$ is the sliding variable defined by (11) and $sgn(.)$ is the sign function defined as

Sgn(S(t))= +1   if S(t)>0
           = -1   if S(t)<0   (14)

Assumtion-2: The gain β must be chosen so that $\beta \geq |x(t)|$ for all time.

When the sliding mode occurs on the sliding surface (12), then, $S(t) = \dot{S}(t) = 0$ and the tracking error $e(t)$ converges to zero exponentially. Finally, the reference torque command T_e^* can be obtained by substituting (13) in (9) as follows.

$$T_e^*(t) = \frac{1}{b}\left[(h.e) - \beta\,\mathrm{sgn}(S) + a\omega_m^* + \dot{\omega}_m^* + d\right]$$

(15)

IV. SIMULATION RESULTS AND DISCUSSION

   To validate the DSVM based direct torque control of induction motor drive using sliding mode speed controller, a numerical simulation has been carried out using Matlab-Simulink platform.. For the simulation, the reference flux is taken as 1wb and starting torque is limited to 15 N-m. The induction motor used in this case study is a 1.5 KW, 1440 rpm, 4-pole, 3-phase induction motor having the following parameters:

R_s =7.83 ohm R_r = 7.55 ohm
L_m = 0.4535 H L_s = 0.475 H; L_r = 0.475 H
J = 0.06 Kg - m^2 B=0.01 N-m.sec/rad

For the proposed integral switching surface sliding mode speed controller, the values of h and β are chosen as h = -200 and β =10. Various conditions are simulated with and without sliding mode speed controller; the results are presented and compared to CDTC. The results for DSVM based DTC are shown in Fig 5.1 to Fig 5.17.

   The starting transients of DSVM based direct torque controlled induction motor drive are shown in Fig 5.1, from which it can be observed that the ripples in starting torque are less when compared to CDTC. The no-load steady state plots of speed, torque, current and stator flux are given in Fig 5.2 and the harmonic spectrum of no-load stator current is shown in Fig 5.3. From Fig 5.1 and Fig 5.3, it can be concluded that the ripples in torque, flux and current can be reduced with the help of DSVM. The d-axis and q-axis stator fluxes and stator flux at no-load steady state condition are given in Fig 5.4 and the locus of stator flux at 1300 rpm is shown in Fig 5.5.

   Fig 5.6 and Fig 5.7 show the speed, torque and current transients responses during the step change in load torque of 10 N-m without and with the proposed sliding mode speed controller. Moreover, the comparison of speed responses is shown in Fig 5.8, from which it can be observed that the speed performance has been improved with the help of proposed speed controller. Also, to validate the proposed controller, another load torque disturbance that consists of both step changes and sinusoidal disturbance as shown in Fig 5.9 has been applied on DSVM based DTC.

   Fig 5.10 and Fig 5.11 show the transient responses during the new load disturbance with out and with the proposed speed controller and the comparison of speed responses is shown in Fig 5.12. From Fig 5.10, it can be observed that for sinusoidal varying load disturbances, the speed response is also varying sinusoidally. From Fig 5.8 and Fig 5.12, it can be concluded that though the load torque is added or removed the speed response is almost the same with the proposed speed controller. Thus, the speed tracking is not affected by the external load torque disturbances. Hence, the proposed speed controller is robust to the variation in load torque disturbances and provides the robustness for the drive.

Fig 5.13 shows the transients in speed, torque and currents during the acceleration period, in which the speed is accelerated from 800 rpm to 1300 rpm. Also, the speed, torque and stator currents transients during the speed reversal (from +1300 rpm to -1300 rpm and from 300 rpm to +1300 rpm) with the proposed speed controller are shown in Fig 5.14 and Fig 5.15. The no-load steady state plots at 600 rpm (region of medium speeds) and 150 rpm (region of low speeds) are shown in Fig 5.16 and Fig 5.17 respectively. If the rotor speed is greater than the half of the rated speed then that speed is consider as high speed, if the motor speed is in between the half of the rated speed and one sixth of the rated speed then that speed is considered as medium speed and if

the speed is below one sixth of the rated speed then the speed is considered as low speed in this paper.
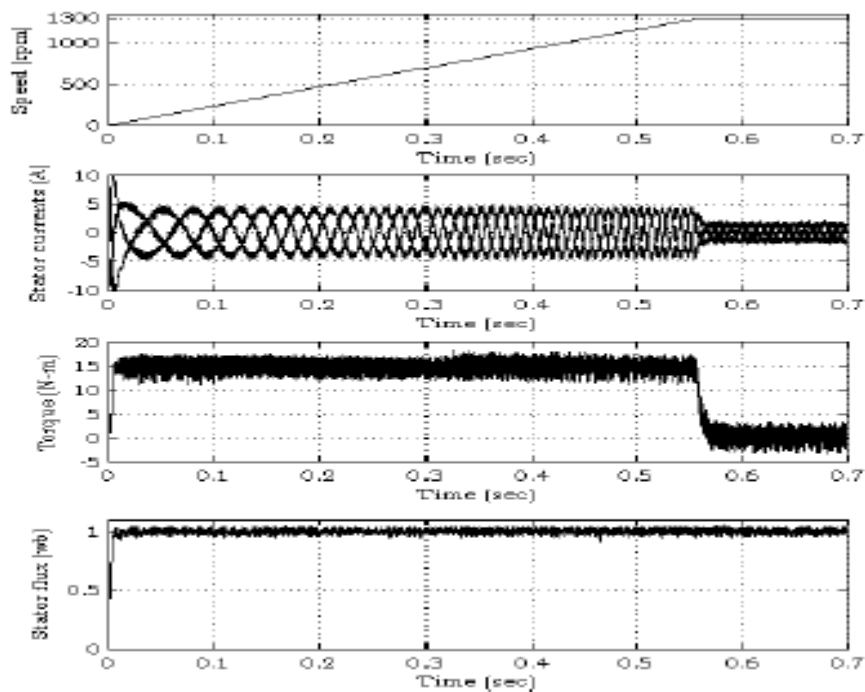

Fig.5.1. DSVM based DTC no load starting transients
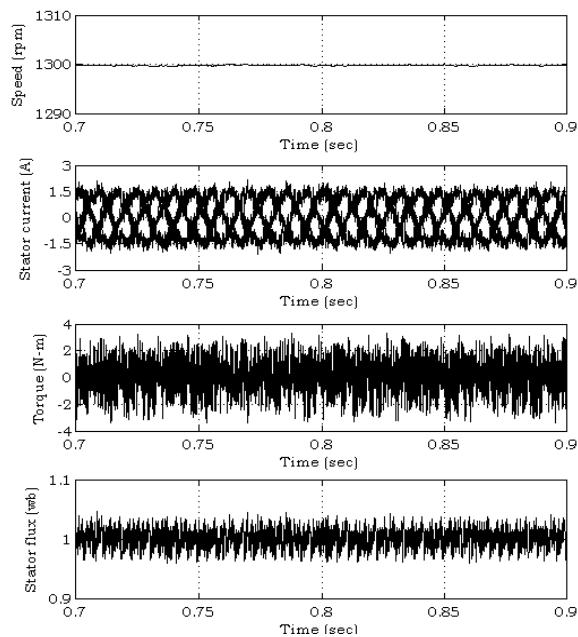

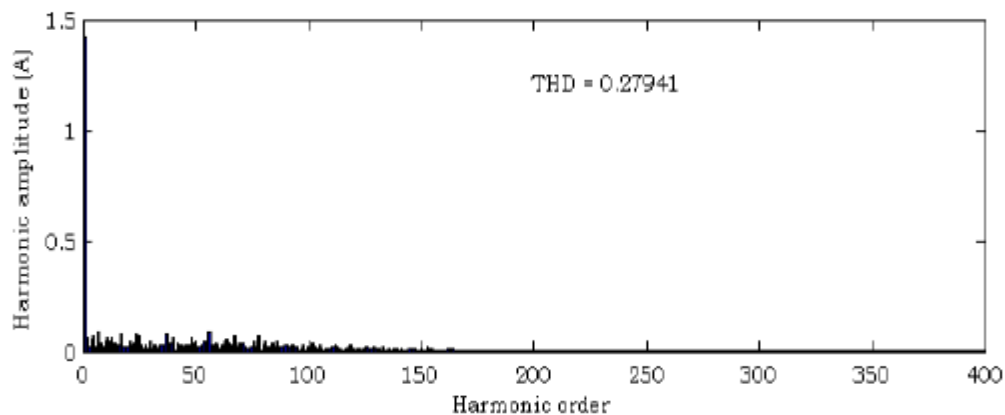Fig.5.2. DSVM based DTC no load steady state plots

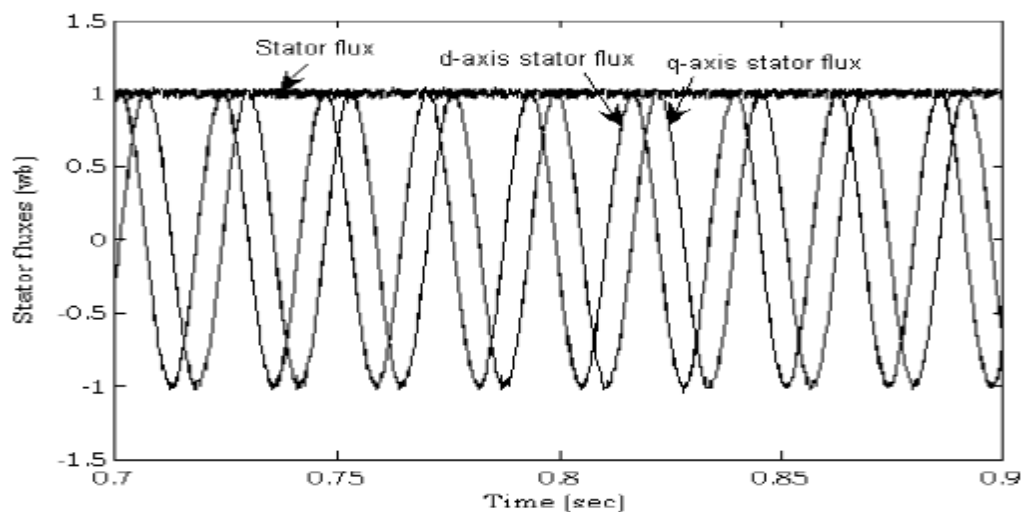Fig.5.3. DSVM based DTC- Harmonic spectrum of stator current

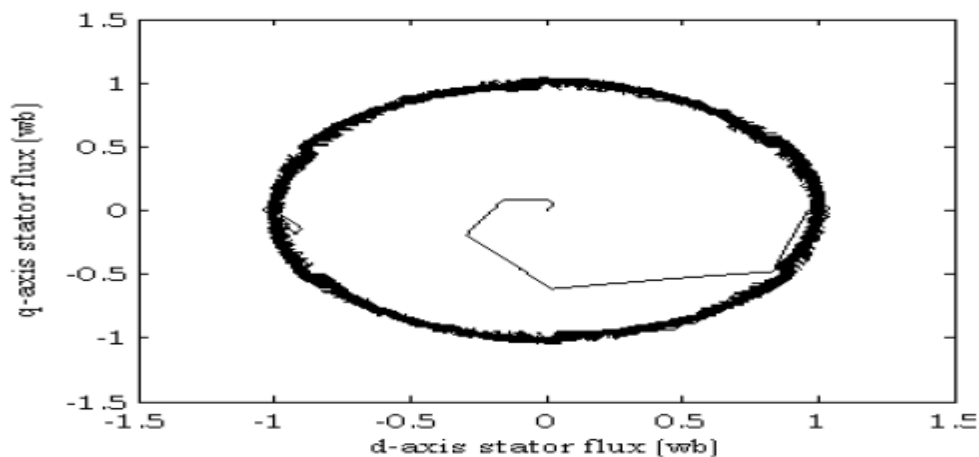Fig.5.4. DSVM based DTC- no load steady state stator fluxes

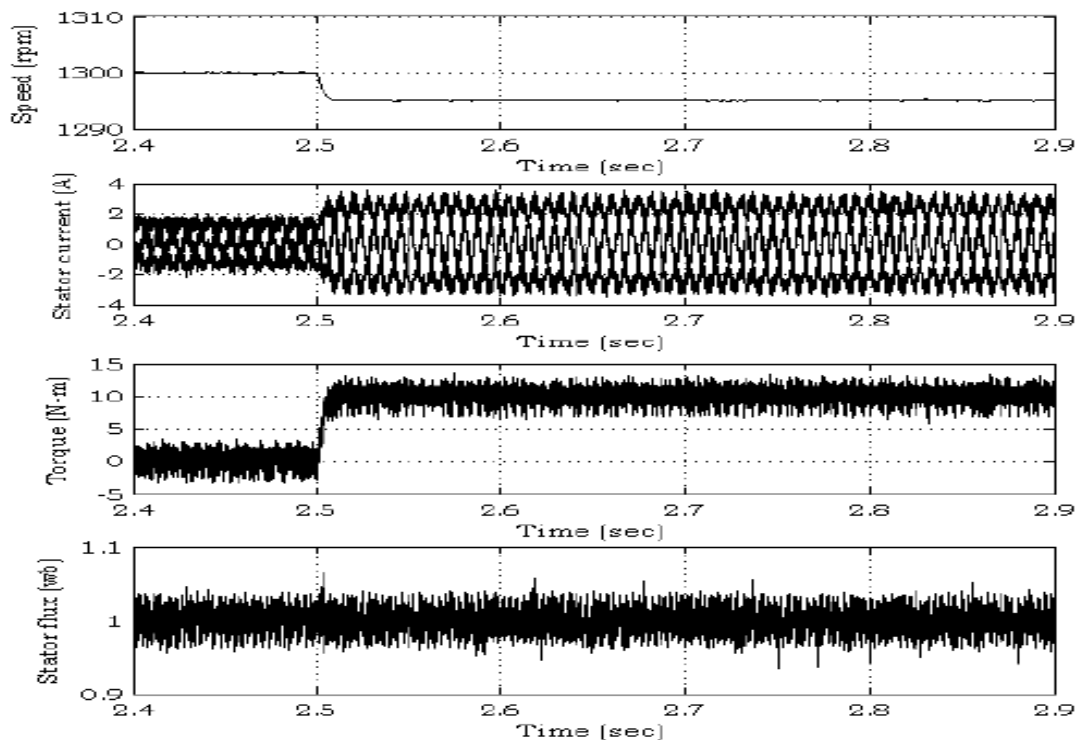Fig.5.5. DSVM based DTC- locus of state stator flux

Fig.5.6. DSVM based DTC-Transients during step change in load without SMC: a 10 N-m load is applied at 2.5sec
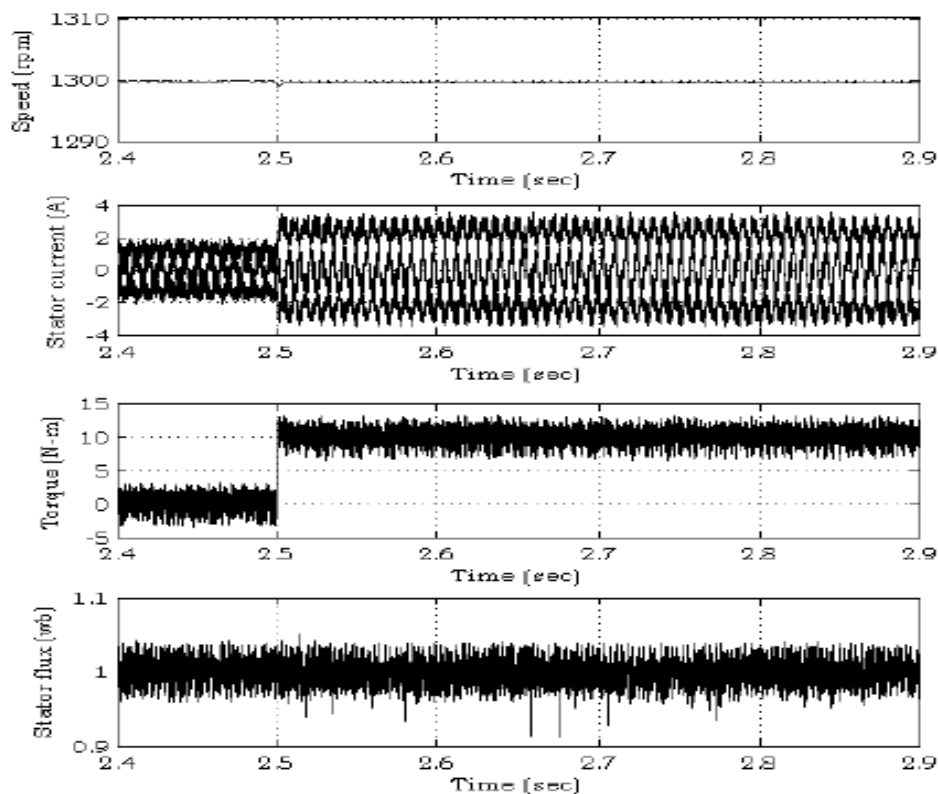
Fig.5.7. DSVM based DTC-Transients during step change in load with SMC: a 10 N-m load is applied at 2.5sec
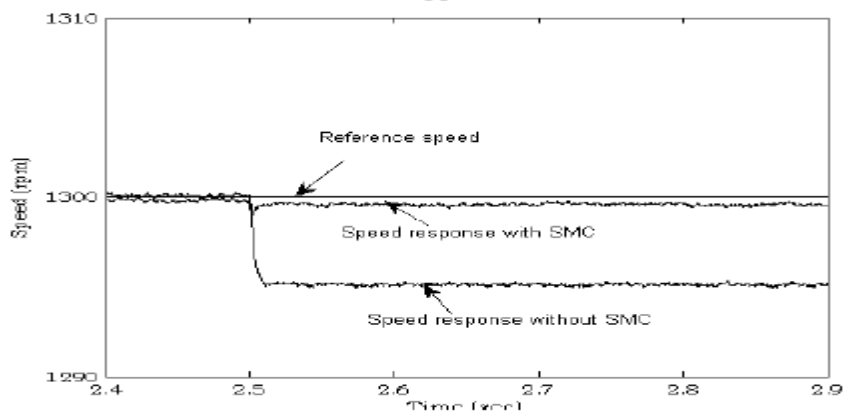
Fig.5.8. Comparison of speed responses during step change in load: a 10 N-m load is applied at 2.5 sec
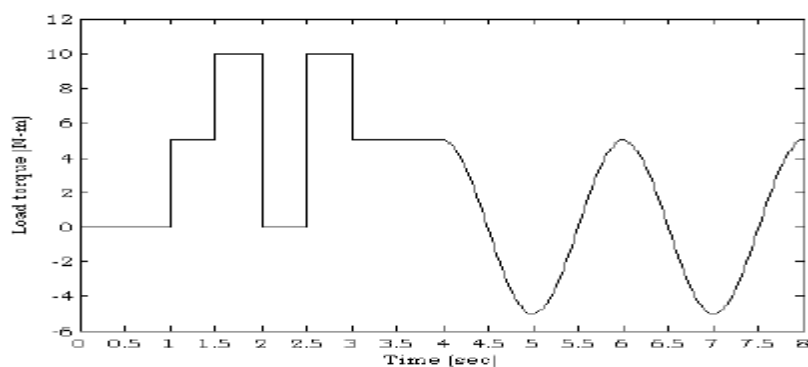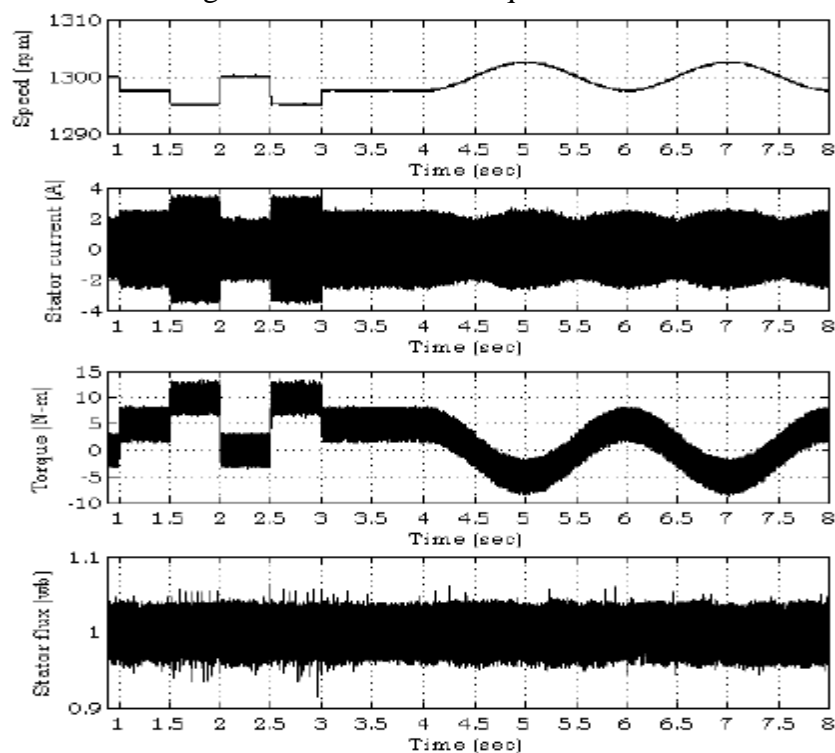

Fig 5.9. External load torque disturbance

Fig 5.10 Transients during external load torque disturbances without SMC
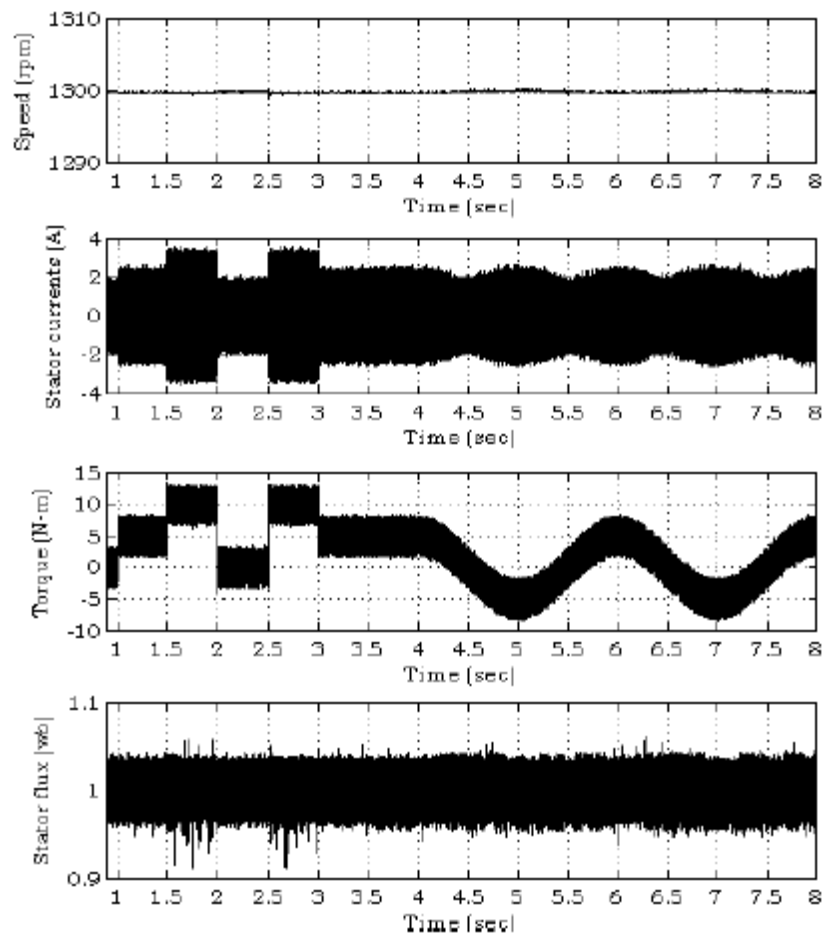
Fig 5.11 Transients during external load torque disturbances with SMC
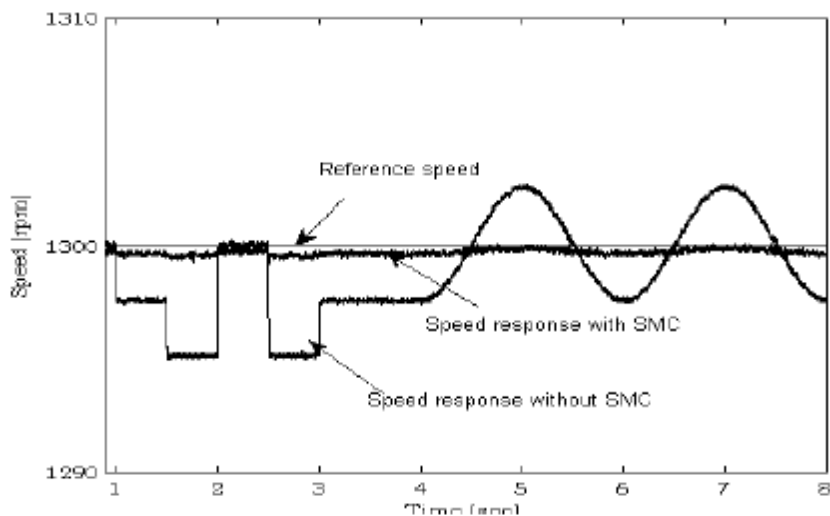

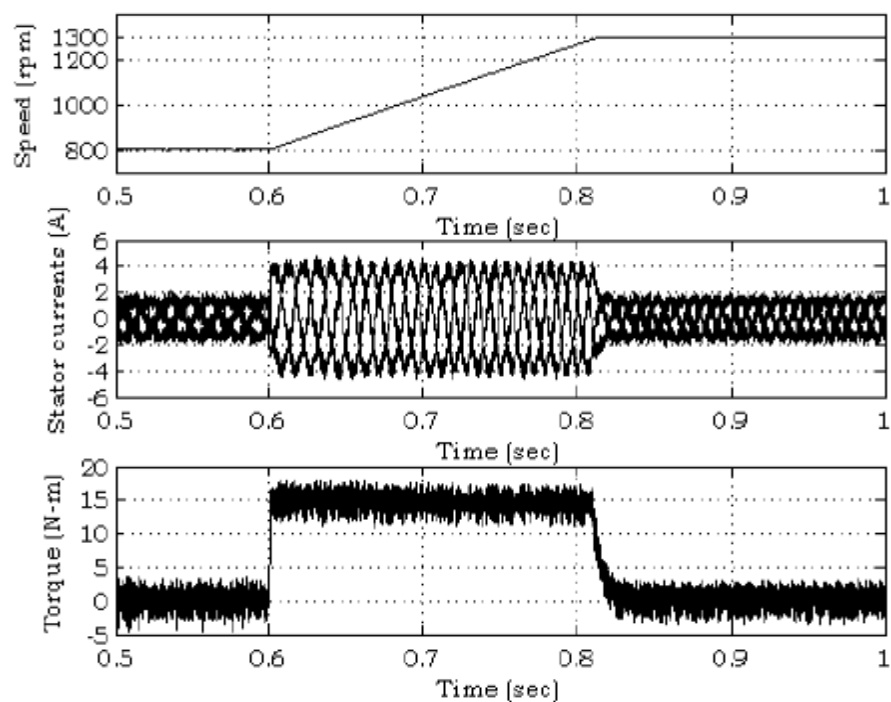Fig. 5.12 Comparison of speed responses during external load torque disturbances

Fig 5.13 Transients during acceleration period: speed is changed from 800 rpm to 1300 rpm at 0.6 sec
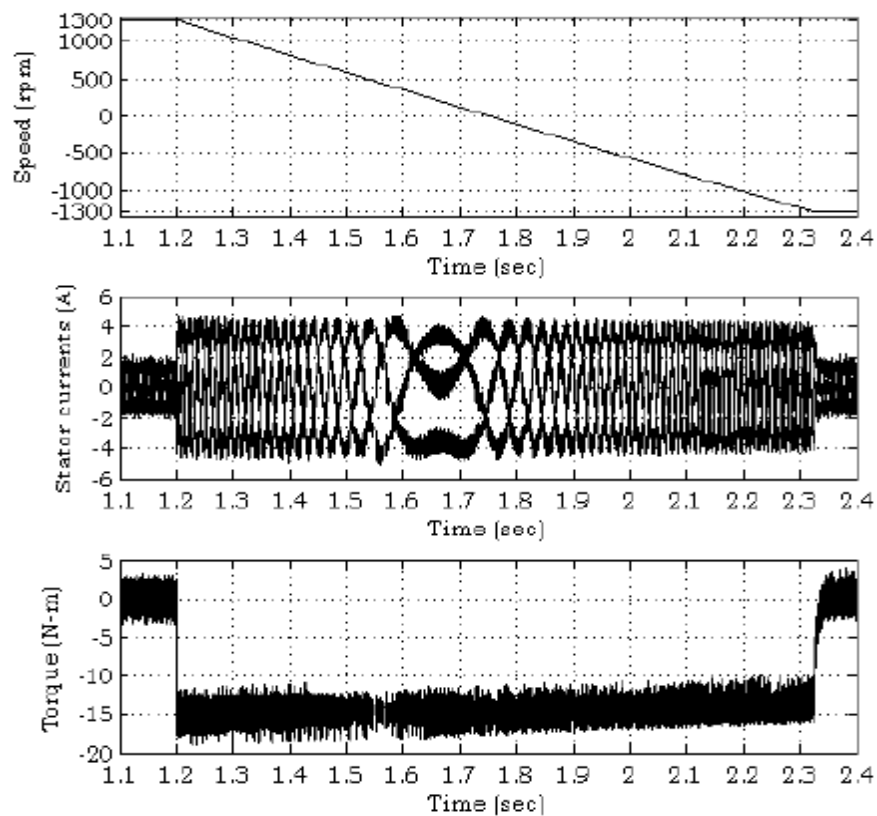
Fig 5.14 Transients during speed reversal: speed is changed from +1300 rpm to -1300 rpm at 1.2 sec
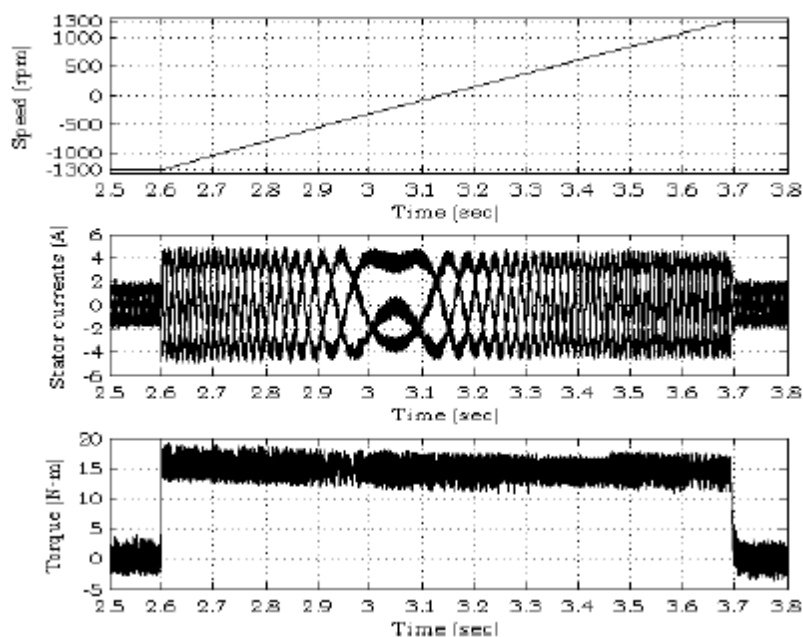

Fig 5.15 Transients during speed reversal: speed is changed from -1300 rpm to +1300 rpm at 2.6 sec
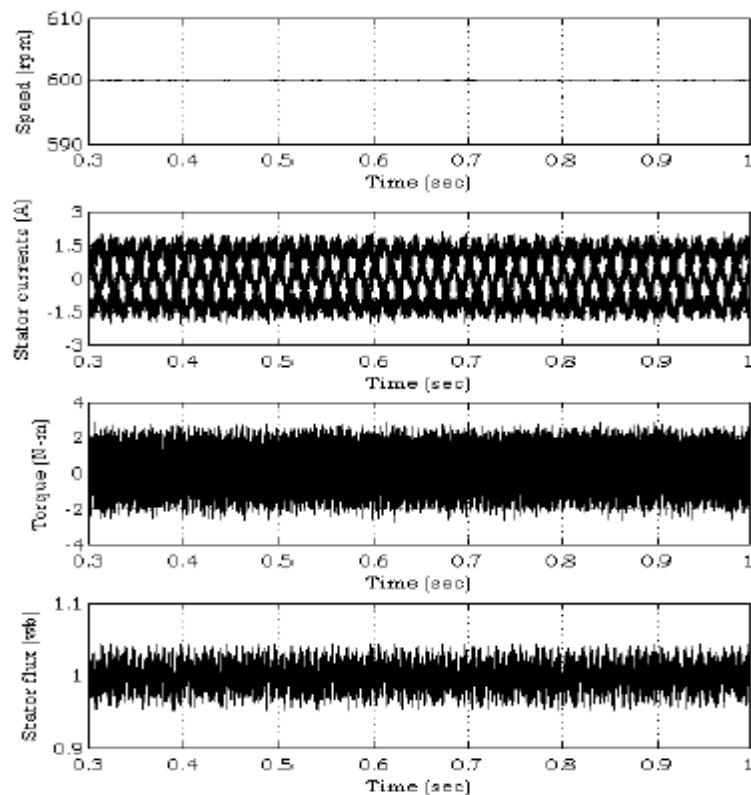
Fig 5.16 DSVM based DTC: no-load steady state plots at 600 rpm
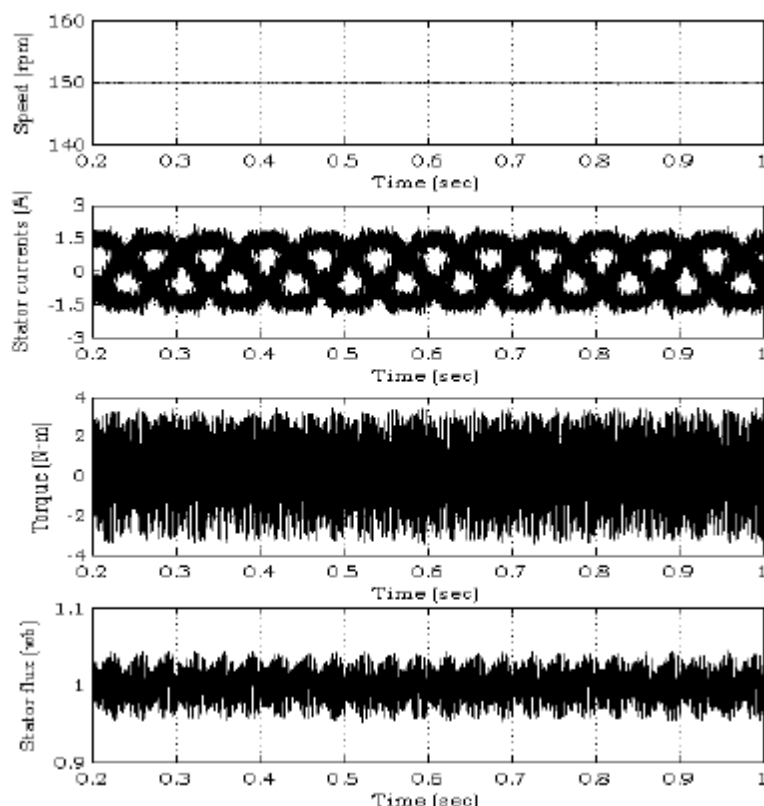(Medium speed region)

Fig 5.17 DSVM based DTC: no-load steady state plots at 150 rpm (Low speed region)

V. CONCLUSIONS

In CDTC, the steady state ripples in current, torque and flux are very high. In order to improve the performance of CDTC in terms of ripples, in this chapter DSVM based DTC has been developed. The DSVM uses prefixed time intervals within a sampling period. Hence, it is possible to synthesize a higher number of voltage vectors with respect to basic DTC scheme. Then, more accurate switching tables have been defined according to the operating speed of induction motor. The DSVM based DTC requires only small increase of the computational time required by the CDTC. By analyzing the flux, current and torque waveforms, it has been shown that the ripples can be reduced with the DSVM method. Also to improve the speed response against the load torque disturbances, an integral switching surface sliding mode speed controller has been used. The simulations at different conditions have been carried out and the results prove the validity of the proposed control algorithm.

REFERENCES

[1] Casadei, F. Profumo, A. Tani, FOC and DTC: two viable schemes for induction motors torque control, IEEE Trans. Power Electron.17(5) (2002) 779–78.

[2] L.H. Hoang, Comparison of field-oriented control and direct torque control for induction

motor drives, in: Conference Recordings of IEEE 34th IAS Annual Meeting, vol. 2, 1999, pp. 1245–1252.

[3] P. Tiitinen, M. Surandra, The next generation motor control method, DTC direct torque control, in: Proceedings on Power Electronics, Drives and Energy Systems for Industrial Growth, vol. 1, 1996, pp. 37–43.

[4] Isao Takahashi, Toshihiko Noguchi, "A new quick response and high-efficiency control strategy of an induction motor", IEEE Trans Ind Appl, Vol.IA-22, No.5, pp. 820-827, Sep/Oct, 1986.

[5] James N. Nash, "Direct Torque Control, Induction Motor Vector Control Without an Encoder", IEEE Trans. Ind. Appl., Vol 33, pp. 333-341, Mar/Apr 1997.

[6] Casadei, G. Grandi, G. Serra, A. Tani, Effects of flux and torque hysteresis band amplitude in direct torque control of induction machines, in: 20th International Conference on Industrial Electronics Control and Instrumentation (IECON), vol. 1, 1994, pp. 299–304.

[7] S. Mir, M.E. Elbuluk, Precision torque control in inverter-fed induction machines using fuzzy logic, in: Proceedings of the 26th IEEE Power Electronics Specialists Conference (PESC), vol. 1, 1995, pp. 396–401.

[8] J.K. Kang, S.K. Sul, New direct torque control of induction motor for minimum torque ripple and constant switching frequency, IEEE Trans. Ind. Appl. 35 (5) (1999) 1076–1082.

[9] Domenico Casadei, Giovanni Serra, Angelo Tani, "Implementation of direct torque control algorithm for induction motors based on discrete space vector modulation" IEEE Trans. PE, Vol.15, No.4, pp. 769-777, July 2000.

[10]R.Toufouti S.Meziane ,H. Benalla, "Direct Torque Control for Induction Motor Using Fuzzy Logic" ICGST Trans. on ACSE, Vol.6, Issue 2, pp. 17-24, June, 2006.

[11]Vadim I. Utkin, "Sliding Mode Control Design Principles and Applications to Electric Drives" IEEE Trans. on Ind. Electronics, vol. 40, no. 1, pp.23-36, Feb 1993.

[12]Kuo-Kai Shyu, Hsin-Jang Shieh, "A New Switching Surface Sliding-Mode Speed Control for Induction Motor Drive Systems", IEEE Trans. P.E, Vol.11, No.4, July 1996.

[13]T. Brahmananda Reddy, J. Amarnath and D. Subba Rayudu, "Direct Torque Control of Induction Motor Based Hybrid PWM Method for Reduced Ripple: A Sliding Mode Control Approach", ICGST Trans. On ACSE, Vol.6, Issue 4, Dec., 2006

D.Veera Bhupal Reddy received B.Tech degree in Electrical and Electronics Engineering from Intell Engineering College, JNTUA, Anantapur in the year 2010. He is currently pursuing M.Tech in G. Pulla- Reddy Engineering College, Kurnool. His research intrests include Electrical Drives.

Dr. T. Brahmananda Reddy was born in 1979. He graduated from Sri- Krishna Devaraya University, Anantapur in the year 2001. He received M.E degree from Osmania University, Hyderabad, India in the year 2003 and PhD from J.N.T.University, Hyderabad in the year 2009. He is presently Professor and Head of the Electrical and Electronics Engineering Department, G. Pulla- Reddy Engineering College, Kurnool, India. He presented more than 65 research papers in various national and international conferences and journals. His research areas include PWM techniques, DC to AC converters and control of electrical drives